

Behaviour of $[\text{PdH}(\text{dppe})_2]\text{X}$ ($\text{X} = \text{CF}_3\text{SO}_3^-$, SbF_6^- , BF_4^-) as Proton or Hydride Donor: Relevance to Catalysis

Michele Aresta,^{*,[a]} Angela Dibenedetto,^[a] Imre Pápai,^[b] Gábor Schubert,^[b] Alceo Macchioni,^[c] and Daniele Zuccaccia^[c]

Abstract: The synthesis, characterization and properties of $[\text{PdH}(\text{dppe})_2]^+$ $\text{CF}_3\text{SO}_3^- \cdot 0.125\text{THF}$ (**1**; dppe = 1,2-bis(diphenylphosphanyl)ethane) and its SbF_6^- (**1'**) and BF_4^- (**1''**) analogues, the missing members of the $[\text{MH}(\text{dppe})_2]^+ \text{X}^-$ ($\text{M} = \text{Ni}, \text{Pd}, \text{Pt}$) family, are described. The Pd hydrides are not stable in solution and can react as proton or hydride donors with formation of dihydrogen, $[\text{Pd}(\text{dppe})_2]^{2+}$ and $[\text{Pd}(\text{dppe})_2]$. Complexes **1–1''** react with carbocations and carbanions by transferring a hydride and a proton, respectively.

Such H^- or H^+ transfer occurs also towards unsaturated compounds, for example, hydrogenation of a C=C double bond. Accordingly, **1** can hydrogenate methyl acrylate to methyl propionate. Complex **1''** is an effective (hourly turnover frequency = 16) and very selective (100%) catalyst for the hydro-

genation of cyclohexen-2-one to cyclohexanone with dihydrogen under mild conditions. Density functional calculations coupled with a dielectric continuum model were carried out to compute the energetics of the hydride/proton transfer reactions, which were used to rationalize some of the experimental findings. Theory provides strong support for the thermodynamic and kinetic viability of a tetracoordinate Pd complex as an intermediate in the reactions.

Keywords: density functional calculations • homogeneous catalysis • hydride ligands • hydrogenation • palladium

Introduction

Transition-metal hydrides are active in a variety of catalytic reactions, and the behaviour of the M–H bond has been the subject of detailed investigations^[1] with the aim of understanding the mode of cleavage of the metal–hydrogen bond, which, in principle, can release a hydride ion,^[2] a hydrogen atom^[3] or a proton.^[4] The relationships between the three paths were clearly discussed by Wayner et al.^[5] in terms of electron-transfer reactions. A concept used to classify M–H bonds has been their “acidity” or “hydricity”.^[6] Cationic hydrides have received particular attention because of their similarity to natural hydrogen-transfer systems such as the

NADP/NADPH⁺ couple. Among cationic hydrides, complexes of formula $[\text{MH}(\text{dppe})_2]^+$ (dppe = 1,2-bis(diphenylphosphanyl)ethane) have long been investigated, and the metals of the Pt family play a leading role as intermediates in a large number of hydrogenation reactions. While the Ni hydride^[7] was prepared in the 1970s and the Pt analogue was more recently extensively investigated,^[6b] the Pd hydride could not be obtained by using the same synthetic methodology as for Ni or Pt. Following our previous studies on the reaction of Pd⁰ complexes with Brønsted acids,^[8] which allowed us to identify in solution the species $[\text{PdH}(\text{dppe})_2]^+$, we investigated in detail the reaction of $[\text{Pd}(\text{dppe})_2]$ with Brønsted acids with the double goal of developing a synthetic methodology of general validity for the isolation of species of formula $[\text{PdH}(\text{dppe})_2]^+$ and to study their properties. We report here the synthesis of $[\text{PdH}(\text{dppe})_2]^+ \text{X}^-$ ($\text{X}^- = \text{CF}_3\text{SO}_3^-, \text{BF}_4^-, \text{SbF}_6^-$) and discuss their structure in solution and the ability to transfer either a proton or a hydride ion to a number of substrates. We also describe the use of the above complexes in hydrogenation reactions in the presence and absence of dihydrogen. Additionally, we use density functional theory along with a dielectric continuum solvent model to provide qualitative information about these reactions, and we examine the structure of a possible intermediate involved in the proton/hydride-transfer processes.

[a] Prof. M. Aresta, Dr. A. Dibenedetto
Department of Chemistry
University of Bari, and CIRCC
via Celso Ulpiani 27, 70126 Bari (Italy)
Fax: (+39)080-544-2429
E-mail: aresta@meta.uniba.it

[b] Dr. I. Pápai, Dr. G. Schubert
Chemical Research Center, Hungarian Academy of Sciences
1525 Budapest, P.O.B. 17 (Hungary)

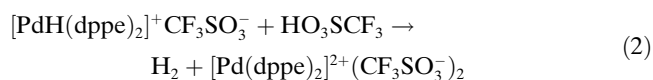
[c] Prof. A. Macchioni, Dr. D. Zuccaccia
Department of Chemistry
Università degli Studi di Perugia
Via Elce di Sotto 8, 06123 Perugia (Italy)

Results and Discussion

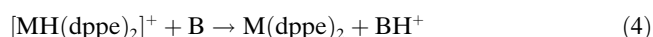
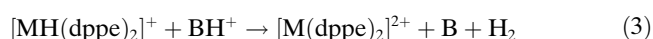
We recently communicated^[9] the synthesis [Eq. (1)] and some solution properties of $[\text{PdH}(\text{dppe})_2]\text{CF}_3\text{SO}_3 \cdot 0.125 \text{ THF}$ (**1**), the missing member of the $[\text{MH}(\text{dppe})_2]\text{X}$ family ($\text{M} = \text{Ni}, \text{Pd}, \text{Pt}$; $\text{dppe} = 1,2\text{-bis}(\text{diphenylphosphanyl})\text{ethane}$).



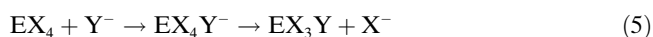
We showed^[9] that **1** can be isolated by operating under the correct reaction conditions and have now extended the preparative methodology to synthesize analogues of **1** such as $[\text{PdH}(\text{dppe})_2]^+\text{X}^-$, where $\text{X}^- = \text{SbF}_6^-$ (**1'**) or BF_4^- (**1''**). The synthetic methodology described here appears to have potentially wide application. It is based on the addition of a stoichiometric amount of the absolutely anhydrous acid to $[\text{Pd}(\text{dppe})_2]$ in THF at 273 K. The cationic hydride separates as a yellow solid and can be isolated by filtration in microcrystalline, pure form. The addition of the acid must be carried out such that accumulation of any excess in solution is avoided. A detailed study on complex **1** clearly showed that, in the presence of free acid, it promptly reacts according to Equation (2) to afford the dicationic complex $[\text{Pd}(\text{dppe})_2]^{2+}(\text{CF}_3\text{SO}_3^-)_2$.



This behaviour is also exhibited by analogous complexes **1'** and **1''**. Our previous DFT QM/MM calculations^[9] showed that the most likely structure of the $[\text{PdH}(\text{dppe})_2]^+$ ion is a capped tetrahedron. We also performed calculations to compare the energy for the H_2 formation [Eq. (3); $\text{M} = \text{Ni}, \text{Pd}, \text{Pt}$; $\text{B} = \text{NH}_3, \text{NEt}_3, \text{CF}_3\text{SO}_3^-$] and found the following trend for the hydride-donor capabilities: $\text{Pd} > \text{Pt} > \text{Ni}$.^[9] The estimated energies of proton transfer from $[\text{MH}(\text{dppe})_2]^+$ [Eq. (4)] indicate that in the Pt family, the most acidic species is that with $\text{M} = \text{Pd}$.^[9]



These data allow the thermodynamic features of the Pt family cationic hydrides to be completed. Also, the reaction of the $18e^-$ species $[\text{Pd}(\text{dppe})_2]$ is a paradigm of a more general class of reactions involving covalent tetrahedral species EX_4 and a nucleophile [Eq. (5), where E is a carbon atom involved in an $\text{S}_\text{N}2$ process] or an electrophile [Eq. (6), where E is a metal center involved in an alkylation or a protonation process].



A pentacoordinate adduct (anionic or cationic) is a common feature of the two processes, and its nature and geometry are still the subject of investigation by theoreticians

with regard to the barriers of interconverting limit structures and the energy of reaction.^[9]

All complexes **1–1''** were characterized in solution by ^1H and ^{31}P NMR spectroscopy. In the ^1H NMR spectrum they show a quintuplet at -7.58 , -7.8 and -7.22 ppm, respectively, attributed to the hydridic hydrogen atom, and in the ^{31}P NMR spectrum (in which the P was allowed to undergo only scalar coupling with the hydridic hydrogen atom), a doublet at 34.48, 34.47 and 34.44 ppm, respectively, attributed to the four equivalent phosphorus atoms. The stability in solution decreases in the order $\mathbf{1''} > \mathbf{1'} > \mathbf{1}$, and the lifetime depends on the temperature and solvent: typically, at 300 K in CH_2Cl_2 it is a few hours for **1''** and roughly one hour for **1**. Therefore, $[\text{PdH}(\text{dppe})_2]^+\text{BF}_4^-$ was further characterized by ^{13}C and ^{19}F NMR spectroscopy at low temperature, as in the time needed for the recording the spectrum no decomposition took place. Conversely, **1** and **1'** under the same conditions start to decompose, so that it is not possible to obtain a clean spectrum, and signal assignment is difficult. The low-temperature NMR study permitted the anion to be located with respect to the cation and any interaction of the former with the Pd–H bond to be excluded. It is noteworthy that even at 225 K the four phosphorus atoms of the coordinated diphos ligands appear to be equivalent, and there is no sign of signal broadening and separation into more structured multiplets, as expected for a rigid structure. Compounds **1–1''** most likely have a capped tetrahedral structure. In such a case, three phosphorus resonances (1:1:2) would be expected in the ^{31}P NMR spectrum. The observed singlet implies a low-energy fluxional process that exchanges the P positions even at 225 K. The magnetic equivalence of the four P arms makes the assignment of resonances rather simple (see Experimental Section). The spatial proximities of Pd–H and *ortho*-H (Figure 1) and of *ortho*-H and CH_2 dppe protons (Figure 2) were established by the ^1H NOESY spectrum.

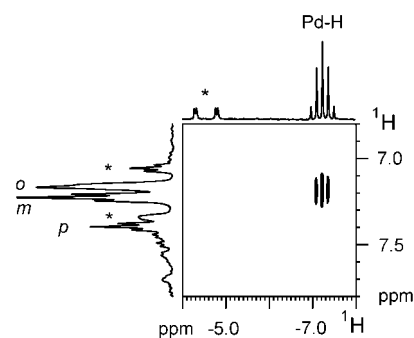


Figure 1. Section of the ^1H NOESY spectrum (400.13 MHz, 225 K, CD_2Cl_2) of **1''** showing the dipolar interaction between Pd–H and *ortho*-H of dppe. Asterisks denote Pd–H resonances of another compound bearing dppe, that is, the complex bearing a monodentate dppe that slowly forms in solution.

The relative anion–cation orientation was investigated by $^{19}\text{F}, ^1\text{H}$ HOESY spectroscopy^[10] with the principal aim of finding any possible interaction between the fluorine atoms of the BF_4^- ion and the PdH moiety that might arise from

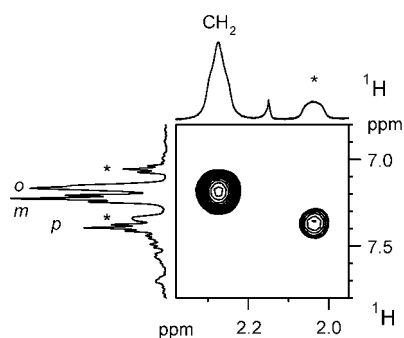


Figure 2. Section of the ^1H NOESY spectrum (400.13 MHz, 225 K, CD_2Cl_2) of **1'** showing the dipolar interaction between the *ortho*-H and CH_2 dppe protons. Asterisks denote resonances of another compound bearing dppe, that is, the complex bearing a monodentate dppe that slowly forms in solution.

possible accumulation of positive charge on the hydrogen atom directly bonded to palladium.

Previous studies have indicated that the anion avoids staying close to "normal" negatively polarized hydridic hydrogen atoms.^[11] The $^{19}\text{F},^1\text{H}$ HOESY NMR spectrum of **1'** shows only weak interionic interactions between BF_4^- and the aromatic protons of dppe (Figure 3). In particular, stron-

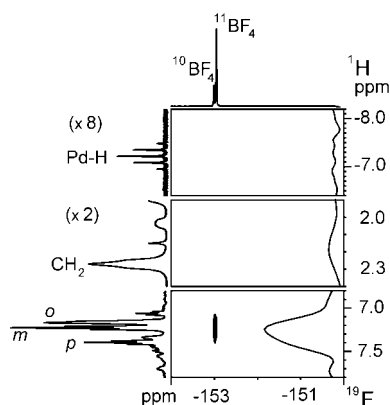
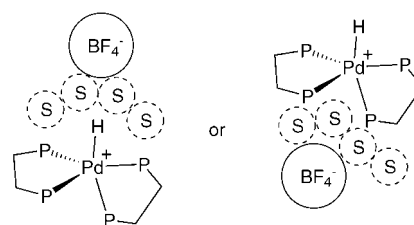


Figure 3. Three sections of the $^{19}\text{F},^1\text{H}$ HOESY NMR spectrum (376.65 MHz, 225 K, CD_2Cl_2) of **1'** showing the interionic interactions between BF_4^- and the dppe aromatic protons. The F1 trace (indirect dimension) relative to the $^{11}\text{BF}_4^-$ resonance is reported on the right.

ger interactions are found with the *meta* and *para* protons.

The $^{19}\text{F},^1\text{H}$ HOESY NMR spectrum does not show any interaction of BF_4^- with Pd–H or with the dppe CH_2 protons (Figure 3). The absence of an interionic interaction between the anion and Pd–H is not a conclusive proof of the nonprotic character of the Pd-bonded H atom, as such an absence could be also due to the intrinsically low intensity of the NOE interaction, which could be masked by the noise.^[12] Conversely, the lack of $\text{BF}_4^-/\text{CH}_2$ interaction and the observation of interionic interactions that are stronger for *meta* and *para* than for *ortho* protons suggest that the anion has little tendency to form intimate ion pairs and indicates two possible anion–cation orientations (Scheme 1).

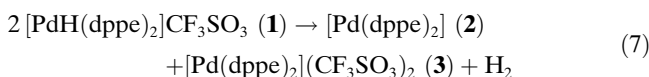
In the first, the anion approaches the cation from the PdH side but remains rather distant from it, due to either



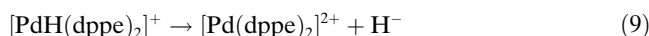
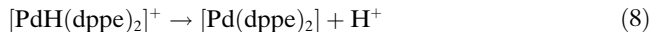
Scheme 1. Possible anion–cation orientations: the anion approaches the cation from the H side (left) or the P side pseudo-*trans* to H (right).

the steric protection exerted by the four phenyl groups pointing above the plane defined by the three phosphorus atoms or the possible interposition of solvent molecules between the anion and the cation (Scheme 1, S=solvent). The second possible anion–cation orientation could involve the approach of the anion from the side of the P arm that stays in pseudo-*trans* position with respect to the Pd–H moiety.

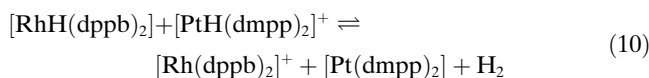
As mentioned above, **1–1'** are labile in solution. In particular, in CH_3CN **1** reacts according to Equation (7).



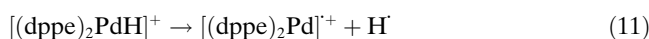
The formation of H_2 and Pd^0 and Pd^{II} species implies that $[\text{PdH}(\text{dppe})_2]\text{CF}_3\text{SO}_3$ must behave as a proton donor affording $[\text{Pd}(\text{dppe})_2]$ (**2**) [Eq. (8)] and as hydride donor affording $[\text{Pd}(\text{dppe})_2](\text{CF}_3\text{SO}_3)_2$ (**3**) [Eq. (9)]. This requires unique properties of the metal hydride that allow it to play a dual role.



Formation of H_2 from hydride species was recently demonstrated to occur in a reaction implying hydrides with different hydride/proton characters [Eq. (10); dppb = 1,2-bis(diphenylphosphino)benzene, dmpp = 1,2(dimethylphosphino)propane].^[13]

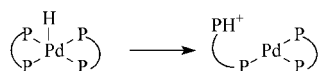


Our Pd complex is thus the first example of a metal hydride that shows amphoteric properties and is able to provide both H^+ and H^- to form H_2 . The mechanism of H_2 formation according to Equation (7) is not yet clear. The formation of H_2 might imply homolytic cleavage of the Pd–H bond to afford an H atom and the radical cation $[(\text{dppe})_2\text{Pd}]^{\cdot+}$ [Eq. (11)], which might catalyze the decomposition of the cationic hydride, as in the case of $[\text{CoH}(\text{CO})_4]$.



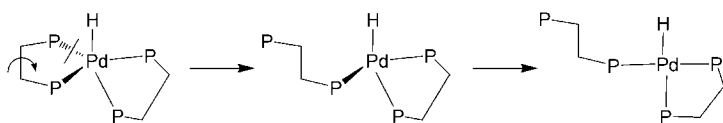
The use of a radical scavenger demonstrated that this path is not likely to occur, as the rate of H_2 formation remains unchanged in presence or absence of the scavenger.

Alternatively, an intramolecular H transfer to a P atom could generate a three-coordinate Pd complex bearing a phosphonium off-arm (Scheme 2), which could intermolecu-



Scheme 2. Intramolecular H transfer with generation of a phosphonium center.

larly react with a second molecule of Pd hydride to afford H_2 . However, such a pathway is not supported by any NMR evidence for formation of a three-coordinate Pd complex bearing a phosphonium group. Instead, we observed that in CH_3CN a new hydride is formed from **1** with an H signal at -4.70 ppm and a $^2J_{\text{PH}}$ typical of a *trans* arrangement (220.4 Hz) (Figure 1). However, such a species is likely to be a four-coordinate $[\text{PdH}(\text{dppe})_2]^+$ intermediate formed by decoordination of one arm of a dppe ligand. To provide support for this assumption, we estimated the energy of opening of the five-membered metallating by carrying out DFT/COSMO calculations on the model compound $[\text{PdH}(\text{dpe})_2]^+$ ($\text{dpe} = 1,2$ -diphosphanylethane). From the global minimum structure of $[\text{PdH}(\text{dpe})_2]^+$, which is a capped tetrahedron, similarly to $[\text{PdH}(\text{dppe})_2]^+$, we constructed an unsaturated species by inverting the PCCP dihedral angle in the dpe ligand perpendicular to the Pd–H bond (Scheme 3).



Scheme 3. Formation of a four-coordinate Pd^+ species from $[\text{PdH}(\text{dppe})_2]^+$.

The geometry optimization for the chelate/opened species yields a square-planar structure (Figure 4) that is only $7.2 \text{ kcal mol}^{-1}$ less stable than the parent compound.^[14] The inclusion of solvent effects by means of COSMO calculations reduces this energy difference to $3.4 \text{ kcal mol}^{-1}$ ($\epsilon = 7.5$ with THF) and $2.9 \text{ kcal mol}^{-1}$ ($\epsilon = 36.6$ with CH_3CN), and this points to the stabilizing role of the solvent medium in the formation of the unsaturated species.

The saddle point connecting the five- and four-coordinate structures on the $[\text{PdH}(\text{dpe})_2]^+$ potential-energy surface is located $9.5 \text{ kcal mol}^{-1}$ above the saturated complex in the gas phase, whereas this barrier is calculated to be only $5.4 \text{ kcal mol}^{-1}$ with the solvated model. These results indicate that opening of the chelate arm is both thermodynamically and kinetically feasible, and that the short-lived intermediate hydride involved in Equation (7) might correspond to the four-coordinate species.

Chelate opening in the hydride complex implies decreasing the electron density on the metal center, since the net σ donation from dppe is reduced by the cleavage of a Pd–P bond. Hirschfeld population analysis of the two structures showed that the net atomic charge on Pd varies from -0.09 to $+0.24$ on dechelation, whereas the slight negative charge

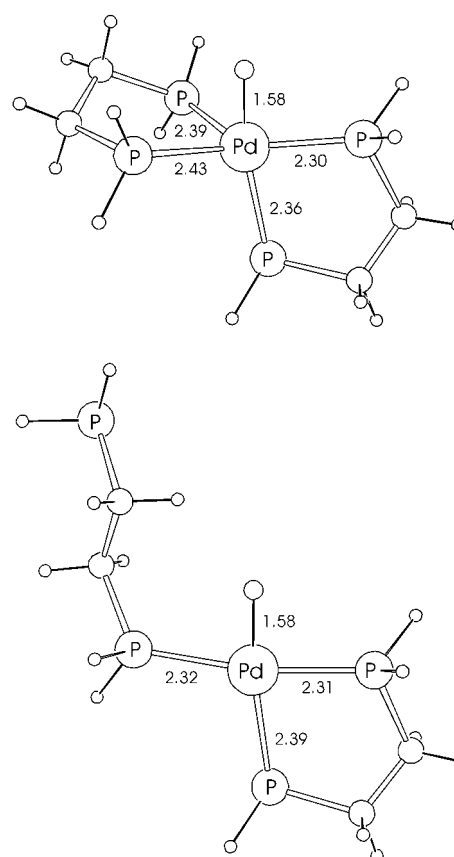
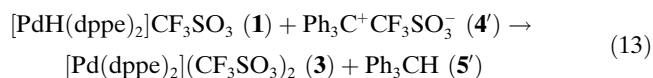
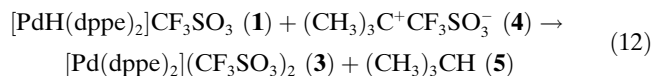


Figure 4. Geometry-optimized structures of the five- and four-coordinate forms of $[\text{PdH}(\text{dpe})_2]^+$ (selected bond lengths in Å).

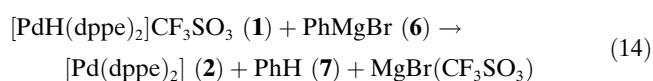
on H (-0.08) remains almost unchanged (becomes -0.09). Overall, the metal–hydride bond becomes more polarized in the four-coordinate intermediate, and this may alter the acidic and hydridic behaviour of the hydride complex. The charge redistribution on the Pd–H bond associated with dechelation is expected to be overestimated by the $[\text{PdH}(\text{dpe})_2]^+$ model relative to the real $[\text{PdH}(\text{dppe})_2]^+$ complex, because the π -acceptor ability of the dppe ligand may partially compensate this effect. Indeed, our calculations on the two forms of the full $[\text{PdH}(\text{dppe})_2]^+$ complexes (single-point BP86/TZP calculations for structures derived by $\text{H} \rightarrow \text{C}_6\text{H}_5$ substitution in our $[\text{PdH}(\text{dpe})_2]^+$ models) gave the following Hirschfeld charges: $Q(\text{Pd}) = -0.10$ and $Q(\text{H}) = -0.04$ for the five-coordinate form, and $Q(\text{Pd}) = -0.03$ and $Q(\text{H}) = -0.03$ for the four-coordinate form. Thus, the more realistic model also predicts a decrease in charge density on Pd–H upon dechelation. These figures suggest that the “one-arm-off” process decreases the negative charge on the Pd–H system, which agrees with the fact that the four-coordinate hydride shows a proton resonance at -4.7 ppm.^[9] Such a species is less stable than the parent compound, and studies are in progress to ascertain the mechanism of formation of H_2 .

To evidence the two different reactivities of $[\text{PdH}(\text{dppe})_2]\text{CF}_3\text{SO}_3$, we separately treated **1** with hydride and proton acceptors, that is, carbocations and carbanions, respectively, and thus confirmed its unique capabilities. When $(\text{CH}_3)_3\text{C}^+\text{CF}_3\text{SO}_3^-$ (**4**; prepared in situ by treating

(CH₃)₃CCl with anhydrous CF₃SO₃Ag) or Ph₃C⁺CF₃SO₃⁻ (**4'**; prepared in a similar way from Ph₃CCl) is treated with **1** in THF, soon after the mixing the reagents, (CH₃)₃CH (**5**) or Ph₃CH (**5'**) is quantitatively formed [Eqs. (12) and (13)], as shown by NMR spectroscopy.



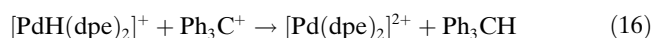
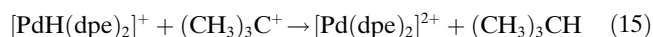
The ¹H and ³¹P{¹H} NMR spectra show the disappearance of the hydride signal of **1** at δ = -7.58 ppm and the conversion of **1** (³¹P signal at δ = 34.54 ppm) to **3** (³¹P signal at δ = 58.35 ppm).^[8,9,15] Conversely, on mixing a solution of **1** in THF with an equimolar amount of PhMgBr (**6**), benzene (**7**) is quantitatively formed [Eq. (14)].



The reaction is very fast, as demonstrated by the immediate disappearance of **1** and formation of the Pd⁰ complex, monitored by carrying out the reaction in a NMR tube and recording the ¹H and ³¹P{¹H} NMR spectra. Concurrently, the hydride signal at δ = -7.58 ppm and the ³¹P signal at δ = 34.54 ppm disappear, while a new ³¹P signal appears at δ = 32.23 ppm, assigned to **2**, as demonstrated by comparison with an authentic sample of [Pd(dppe)₂].

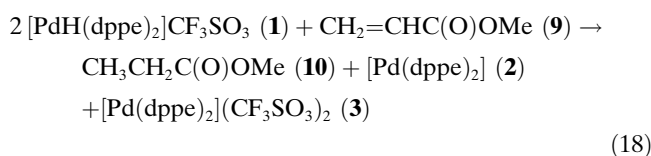
Macroscopically, the proton transfer appears to be as fast as the hydride transfer. In both cases, the reaction is very selective, without any formation of by-products.

In an attempt to provide some rationale for our observations, we estimated the energy balance for the model reactions given in Equations (12)–(14) by carrying out DFT/COSMO calculations, taking into account only the Pd hydride cation (represented by [PdH(dppe)₂]⁺) and the carbanion or carbocation reaction partner [Eqs. (15), (16), and (17)].



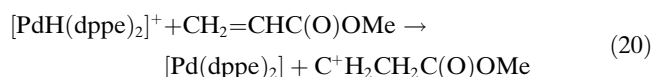
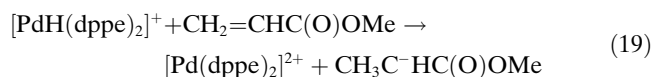
The predicted reaction energies of model reactions 12'/12a' and 13' of -46/-33 and -76 kcal mol⁻¹, respectively, indicate that: 1) proton transfer from [PdH(dppe)₂]⁺ to Ph⁻ is thermodynamically more favourable than hydride transfer to (CH₃)₃C⁺ or Ph₃C⁺ and 2) the nature of the carbocation may strongly influence the energetics of the hydride-transfer reaction. The predicted energetics support the experimental findings and the fact that **1** can act as a proton- or hydride-transfer agent. More detailed mechanistic investigations at the molecular level are required for providing a full interpretation of our experimental observations. Theoretical work is in progress along these lines.

An interesting issue emerged at this point, that is, to ascertain whether H⁻/H⁺ transfer could be performed with a single substrate as acceptor. Therefore, we treated **1** with methyl acrylate CH₂=CHCOOMe (**9**). The choice of the olefin was not casual. In fact, it is well known that Pd^{II} complexes added with inorganic acids in presence of phosphane ligands are catalysts for the dimerization of **9**^[15,18] to afford either C₆ (T–T coupling) or C₅ (H–T coupling) skeletons, depending on the reaction conditions. Therefore, **1** could act either as H⁺/H⁻ transfer agent or as an oligomerization catalyst. The reaction of **1** with **9** was carried out in parallel in bulk and in an NMR tube, where it was followed by ¹H and ³¹P{¹H} NMR spectroscopy. The ¹H NMR spectrum of the reaction mixture clearly showed the disappearance of the hydride signal at δ = -7.58 ppm and the growth of new signals at δ = 1.03 (CH₃), 2.25 (CH₂) and 3.60 ppm (OMe), assigned to the resonances of methyl, methylene and methoxyl groups of CH₃CH₂C(O)OMe (**10**), respectively. Additionally, the ³¹P{¹H} NMR spectrum shows the formation of Pd⁰ (δ = 32.23 ppm) and Pd²⁺ (δ = 58.35 ppm) species. These data clearly show that **1** act as a donor of hydride and proton to the C=C double bond with formation of the saturated species (**10**) [Eq. (18)].



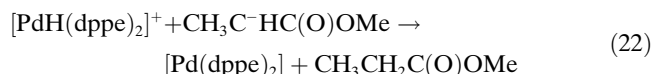
Methyl propionate was also monitored by GC-MS and compared with an authentic sample. Additionally, neither organometallic species derived from the potential interaction of the olefin with the metal center nor dimers of methyl acrylate were detected by NMR spectroscopy. It is noteworthy that formation of H₂ was not observed in this case, in contrast to Equation (3). The formation of **10** can in principle occur in two ways: 1) by sequential or concomitant addition of H⁺ and H⁻ to the double bond and 2) preliminary formation of H₂ according to Equation (3) and subsequent hydrogenation of **9** promoted by Pd^{II} or Pd⁰ species. To exclude that H₂ is involved in the hydrogenation of **9**, we added the olefin and H₂ to the Pd⁰/Pd²⁺ mixture obtained from the stoichiometric hydrogenation of **9** according to Equation (18). Under the same conditions (time, solvent, temperature) used for the reaction of **1** with **9** (293 K), the Pd⁰/Pd²⁺ couple was not able to hydrogenate methyl acrylate. This supports the picture of proton and hydride transfer in the reaction of **1** with methyl acrylate, rather than preliminary formation of H₂ that subsequently adds to **9**. The reaction given in Equation (18) is very clean and **10** is formed as the sole organic product. The hydrogenation of methyl acrylate by **1** by H⁺ and H⁻ transfer is reminiscent of the mechanism of hydrogenation of the C=O group by [RuCl₂(PR₃)₂(NH₂CH₂CH₂NH₂)] complexes, assisted by an alcohol and a base, as described by Noyori.^[19] In both cases, H⁺ and H⁻ are transferred by a mechanism in which the double bond may not be coordinated to the metal, and this suggests that its coordination to the metal atom may not be

a necessary prerequisite for hydrogenation to occur. Comparing our system with that of Noyori, it is remarkable that in our case H^+ and H^- are provided by the same metal center. Either a simultaneous interaction of two Pd–hydride moieties with the double bond or a nearly stepwise mechanism can operate. The former seems to be less favorable for steric reasons if the cationic moiety remains unchanged during the reaction. Assuming a quasi-stepwise mechanism, to determine whether there is any thermodynamic preference for the hydride- or the proton-transfer process in the hydrogenation of **9**, we carried out DFT/COSMO $_{\epsilon=7.5}$ calculations on the species involved in the reaction given in Equation (18) and found that the overall reaction is exothermic by 24 kcal mol $^{-1}$. Assuming that hydride transfer and the proton transfer in the hydrogenation process occur in separate but close steps, one can formally decompose the reaction energy according to whether hydride or proton transfer takes place first. A population analysis on the gas-phase equilibrium structure of **9** indicated an excess of positive partial charge on the terminal CH_2 group, whereas the carbon atom α to the carboxyl group carries a negative charge. One can therefore envision that the first step of the hydrogenation could be Equations (19) or (20).



Our calculations reveal that both reactions are thermodynamically uphill, but the hydride transfer [Eq. (19)] is notably less endothermic ($\Delta E = +26$ kcal mol $^{-1}$) than the proton transfer ($\Delta E = +59$ kcal mol $^{-1}$), that is, the formation of $C^+H_2CH_2C(O)OMe$ is thermodynamically less feasible than the formation of the anionic species.

Moreover, the carbanion resulting from H^- addition, $CH_3C^-HC(O)OMe$, may be stabilized by resonance delocalization of the negative charge [Eq. (21)] which then reacts with **1** that behaves as proton donor to afford the saturated methyl ester [Eq. (22); $\Delta E = -50$ kcal mol $^{-1}$].



The sum of reactions in Equations (19) and (22) represents the hydrogenation of methyl acrylate [Eq. (18)] in an exothermic process ($\Delta E = -24$ kcal mol $^{-1}$).

The experimental data reported above are a clear demonstration that the Pd hydride **1** can behave as ambivalent

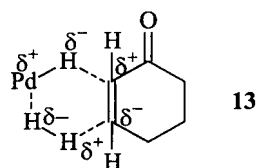
transfer agent of proton or hydride and is also able to transfer both H^+ and H^- to the same substrate, as in the hydrogenation of methyl acrylate.

As the implication of such reactions in catalysis is quite intriguing, we also investigated the behaviour of **1**, **1'** and **1''** towards cyclohexene-2-one (**11**) under H_2 atmosphere or in the presence of 2-propanol as H_2 source under dinitrogen. We found that the alcohol readily transfers a proton to the Pd–H bond of **1** and its congeners with H_2 elimination and formation of a dark Pd species (most likely Pd black). Any eventual hydrogenation activity under these conditions cannot be attributed to the Pd hydride, but more likely to Pd 0 species (Pd metal). Conversely, the addition of H_2 under controlled thermal conditions (below 333 K) does not decompose the hydride complexes **1–1''**, which thus can act as hydrogenation catalysts without formation of Pd black, as determined at the end of the hydrogenation run. Compound **11** has two different sites of reaction: the C=C double bond and the C=O group. From a kinetic point of view, most probably the hydrogenation of the two moieties starts with a different step: hydride transfer to C in the former case, and a proton transfer to O in the latter. Moreover, if the hydrogenation process were thermodynamically controlled (our DFT/COSMO calculations ($\epsilon = 7.5$) predict cyclohexanone to be 13 kcal mol $^{-1}$ more stable than cyclohexen-2-ol), hydrogenation of the double bond ($\Delta G = -25.9$ kcal mol $^{-1}$) should preferentially occur over hydrogenation of the keto group (-12.9 kcal mol $^{-1}$). The latter would imply as a first step proton transfer to the keto oxygen atom. Although all complexes **1–1''** exhibit the same behaviour, we discuss below the results obtained with **1''**. Most entries in Table refer to **1''**, which is more stable and allowed the reactive system to be analyzed for a longer time. The reaction of **1** with **11** under 0.1 MPa of H_2 at 297 K (entry 0, Table 1) does not afford any hydrogenated product. If the H_2 pressure is raised to 4 MPa (entry 1), **11** is hydrogenated. At 323 K (entries 3–5) the hourly turnover frequency (TOFh) increases, and cyclohexanone (**12**) is obtained very selectively. Neither cyclohexen-2-ol nor cyclohexanol was found in the reaction mixture. Increasing the temperature from 323 to 340 K increases the TOFh, which reaches the best value of 95. Nevertheless, while at 323 K the cationic H–Pd complex is recovered at the end of the run, at 340 K **1** slowly decomposes to dark Pd species that also are very good catalysts for the hydrogenation of **11** (entries 6–8). Complexes **1** and **1'** show lower TOFh than **1''** at 323 K, and this agrees with the fact that they have a shorter lifetime (see above). The TOFh of the Pd black formed by decomposition of **1**, **1'** or **1''** at 350 K is very similar. Its behaviour is comparable with that of Pd–C (5% Pd), which shows a TOFh between 100 and 1000.

The behaviour of **1** and its congeners as catalysts of hydrogenation of **11** and their TOF values raises the question of the reaction mechanism. The fact that no reaction occurs at 0.1 MPa of H_2 indicates that the concentration of H_2 in solution may be the key for the reaction to occur. Under the correct operating conditions, with a fair concentration of hydrogen in solution, the hydride complexes show a catalytic activity that is different from that of the couple Pd $^{2+}$ /Pd 0 .

Table 1. Hydrogenation of cyclohexene-2-one to cyclohexanone.

	Cyclohexen-2-one [mol]	Catalyst [mol]	<i>T</i> [K]	<i>t</i> [h]	<i>P</i> _{H₂} [MPa] or 2-propanol [μL]	TOFh
0	2.00 × 10 ⁻⁵	2.07 × 10 ⁻⁵ (1)	297	20	0.1 MPa	0
1	2.07 × 10 ⁻⁵	2.07 × 10 ⁻⁵ (1)	297	21	4 MPa	0.01
2	1.40 × 10 ⁻⁴	1.43 × 10 ⁻⁵ (1)	323	1	13 μL	–
3	1.38 × 10 ⁻³	1.40 × 10 ⁻⁵ (1)	323	1	4 MPa	2.0
4	1.54 × 10 ⁻³	1.54 × 10 ⁻⁵ (1)	323	1	4 MPa	1.5
5	1.41 × 10 ⁻³	1.41 × 10 ⁻⁵ (1)	323	1	4 MPa	15.9
6	4.80 × 10 ⁻⁵	4.68 × 10 ⁻⁵ (1)	340	1	4 MPa	95.0
7	2.78 × 10 ⁻⁴	2.80 × 10 ⁻⁶ (1)	340	1	4 MPa	95.0
8	2.70 × 10 ⁻³	2.70 × 10 ⁻⁶ (1)	340	1	4 MPa	92.0
9	4.70 × 10 ⁻³	4.70 × 10 ⁻⁶ (Pd/C 5%)	340	1	4 MPa	ca. 1000



Tentatively, we propose the formation of the six-membered adduct **13** as the active hydrogenation intermediate.

Intermediacy of **13** may explain how **11** is hydrogenated to **12**, leaving **1** unchanged. Most likely, for steric reasons, the four-coordinate Pd hydride is involved in such a reaction, rather than the parent five-coordinate complex. It is worth emphasizing that we carefully monitored the reaction system, and, for determining the TOFh of **1** and its congeners, considered only the time during which the reaction solution remained pale yellow without any formation of Pd-black species.

Conclusion

[PdH(dppe)₂]X (X = CF₃SO₃⁻, SbF₆⁻, BF₄⁻) react as hydride or proton donors to carbocations or carboanions, respectively. In solution, they can also generate hydrogen plus Pd²⁺ and Pd⁰ complexes. The H⁺/H⁻ transfer also occurs towards unsaturated organic compounds, for example, methylacrylate to afford, very selectively, methyl propionate. This is the first documented example of a hydride complex acting as a donor of either H⁺ or H⁻. In the presence of dihydrogen, the [PdH(dppe)₂]⁺ ion behaves as a hydrogenation catalyst for cyclohexene-2-one with TOFh = 16 below 323 K. Above this temperature, the hydride decomposes to Pd-black species that also are very active and selective hydrogenation catalysts. Theoretical calculations showed that a four-coordinate Pd–H complex may be the active intermediate in a number of reactions. Studies are in progress to extend knowledge of the properties of the cationic hydride and its applications.

Experimental Section

Air-sensitive compounds were handled under nitrogen with a vacuum/inert gas manifold. FTIR spectra were recorded by using a Bruker 113V Fourier transform interferometer. GC and MS analyses were performed with a Shimadzu QP 5050 GC-MS. NMR spectra were measured with Varian 200 XL, Bruker Avance DRX 400 or Bruker AM 500 instruments. The NMR measurements with the Bruker Avance DRX 400 were performed at 400.13 MHz (¹H), 376.65 MHz (¹⁹F), 161.98 MHz (³¹P) and

100.61 MHz (¹³C). With the Bruker AM 500 the NMR measurements were performed at 500.38 MHz (¹H) and 125.76 MHz (¹³C). All solvents were dried and distilled under dinitrogen as described in the literature.^[20]

Computational details: The reaction energies were estimated from DFT/COSMO calculations carried out for the relevant reactant and product compounds with the ADF program package.^[17a] The dppe (Ph₂PCH₂CH₂PPh₂) ligand in the palladium complexes was replaced with H₂P(CH₃)₂PH₂ (dpe). The structures of all molecules and model complexes were fully optimized in the gas phase at the BP86/TZP level of theory, and first-order quasirelativistic corrections were included in the calculation of binding energies.

Since the reactions considered here involve charged species, inclusion of solvent effects is unavoidable to predict reasonable energetics. The solvation energies were calculated in terms of the conductorlike screening model (COSMO)^[17b] as implemented in ADF. The van der Waals atomic radii, which define the molecule-shaped cavity in the dielectric medium, were chosen as follows: Pd: 1.63, P: 1.8, C: 1.7, O: 1.52, H: 1.2 (all values in Å). We used ε = 7.5 and ε = 36.6 for the dielectric constant of the medium to model the solvents THF and CH₃CN generally used in the experiments. The effect of ion pairing, that is, the presence of counterions (e.g., CF₃SO₃⁻) in the solution, was not considered in our calculations. The energy values reported in the paper refer to *T* = 0 K and do not include zero-point energy corrections.

The applicability of density functional theory coupled with dielectric continuum methods in thermochemistry of reactions involving differently charged species has not been systematically studied, but there are a few examples in the recent literature which indicate the relevance of the present methodology in providing reasonable energetics for proton- or electron-transfer reactions.^[21,22] Our preliminary results for a series of protonation reactions relevant to the present study^[23] show that the computational model applied here gives protonation energies to within about 10 kcal mol⁻¹ as compared to experiment.

The approximation made in our model to stay within reasonable computational cost, that is, the replacement of the dppe ligand by dpe, calls for caution regarding the absolute values of the reported reaction energies. However, all our conclusions based on the calculated energies refer either to analogous reactions, for which the errors introduced by the above simplification are cancelled, or to a set of reactions for which the calculated energies differ by at least 20 kcal mol⁻¹, which is quite likely beyond the error of predictions.

Characterization of [PdH(dppe)₂]BF₄—¹H NOESY and ¹⁹F,¹H HOESY experiments: Gradient pulses, only along the *z* direction, were generated by using the Great 1/10 gradient unit. Sample temperature was controlled with the BVT 3000 variable-temperature unit equipped with digital control; the value was checked by using a 4% CH₃OH in CD₃OD standard tube. Proton, carbon, phosphorus and fluorine spectra were acquired with the 5 mm QNP probe. Chemical shift are relative to external TMS for ¹H and ¹³C, external H₃PO₄ for ³¹P and external CCl₃F for ¹⁹F. All FIDs for proton, fluorine and phosphorus were acquired using 32k or 64k points; the FIDs for carbon spectra were acquired with 64k or 128k data points. Carbon and phosphorus spectra were acquired with decoupling of the ¹H nucleus. In the 2D NMR experiments, the number of digital points dedicated to direct and indirect dimensions was fixed according to the desired resolution and to the total experimental time. Each transient (direct dimension) was acquired with 1k, 2k or 4k points; the number of transients (indirect dimension) varied from 512 to 2k; the number of scans was set at 16, 24 or 32, depending on solute concentration. All two-dimensional spectra were transformed by using the zero filling procedure in both dimensions. The ¹H NOESY^[24] NMR experiments were acquired by the standard three-pulse sequence or by the PFG version.^[25] Two-dimensional ¹⁹F,¹H HOESY NMR experiments were acquired using the

standard four-pulse sequence or the modified version.^[26] Semiquantitative spectra were acquired using a 1 s relaxation delay and 800 ms mixing times.

Synthesis of [PdH(dppe)]₂(CF₃SO₃)₂ (1): Strictly anhydrous CF₃SO₃H (21 μL, 0.242 mmol) was added to a yellow solution of [Pd(dppe)₂] (0.219 g, 0.242 mmol) in anhydrous THF (25 mL), prepared under dinitrogen at 293 K, and the resulting mixture was stirred at 273 K for 3 h, during which a yellow solid formed. The solution was concentrated and the yellow solid collected by filtration under dinitrogen, washed with anhydrous THF (3 × 2 mL), dried in vacuo and characterized as [PdH(dppe)]₂⁺CF₃SO₃⁻·0.125 THF. Yield: 0.180 g, 0.170 mmol, 70.0%; elemental analysis calcd (%) for C₅₃H₄₉F₉O₃P₄SPd·0.125 THF (1063.36): C 59.86, H 4.64, P 11.65, Pd 10.00, S 3.01; found: C 60.27, H 4.97, P 11.49, Pd 10.07, S 2.84; IR (Nujol, KBr disks): $\tilde{\nu}$ = 1916 (νPd–H), 1268 (ν_{as}SO₃), 1223 (ν_sCF₃), 1143 (ν_{as}CF₃), 1030 (ν_sSO₃), 871, 818, 742, 694 (CH₂ rocking vibrations of diphosphane ligands), 637, 571, 518 cm⁻¹ (SO₃ deformations); ¹H NMR (500 MHz, CD₂Cl₂, 293 K): δ = -7.58 (qm, ²J_{H-P} = 54.4 Hz, 1H), 2.28 (brs, 8H, Ph₂PCH₂CH₂PPh₂), 7.24 (m, 32H, *o*- and *m*-dppe), 7.40 ppm (t, 8H, *p*-dppe); ³¹P{¹H} NMR (202.48 MHz, CD₂Cl₂, 293 K): δ = 34.48 ppm (d, ²J_{P-H} = 54.4 Hz).

Synthesis of [PdH(dppe)]₂SbF₆ (1′): A solution of [Pd(dppe)₂] (0.153 g, 0.169 mmol) in THF (25 mL) was prepared under dinitrogen at 293 K, and anhydrous HFSbF₆ (14 μL, 0.169 mmol) was added. The reaction mixture was stirred at 273 K for 3 h and then concentrated under vacuum. The yellow solid was collected by filtration under dinitrogen, washed with anhydrous THF (3 × 2 mL), dried in vacuo and characterized as [PdH(dppe)]₂SbF₆. Yield: 0.157 g, 0.137 mmol, 81.2%; elemental analysis calcd (%) for C₅₂H₄₉F₆P₄SbPd (1140.02): C 54.78, H 4.33, P 10.86, Pd 9.33; found: C 54.25, H 4.68, P 11.02, Pd 9.17. IR (Nujol, KBr disks): $\tilde{\nu}$ = 1913 (νPd–H), 871, 819, 743, 694, 658 cm⁻¹ (CH₂ rocking vibrations of diphosphane ligands); ¹H NMR (500 MHz, CD₂Cl₂, 293 K): δ = -7.8 (qm, ²J_{H-P} = 39.5 Hz, 1H), 2.28 (brs, 8H, Ph₂PCH₂CH₂PPh₂), 7.24 (m, 32H, *o*- and *m*-dppe), 7.40 ppm (t, 8H, *p*-dppe); ³¹P{¹H} NMR (202.48 MHz, CD₂Cl₂, 293 K): δ = 34.47 ppm (d, ²J_{P-H} = 39.5 Hz).

Synthesis of [PdH(dppe)]₂BF₄ (1′′): HBF₄·Et₂O (36 μL, 0.263 mmol) was added to a yellow solution of [Pd(dppe)₂] (0.238 g, 0.263 mmol) in anhydrous THF (25 mL) under dinitrogen at 293 K. The resulting mixture was stirred at 273 K for 3 h. The solution was concentrated and the yellow solid was collected by filtration under dinitrogen, washed with anhydrous THF (3 × 2 mL), dried in vacuo and characterized as [PdH(dppe)]₂BF₄. Yield: 0.210 g, 0.211 mmol, 80.2%; elemental analysis calcd (%) for C₅₂H₄₉BF₄P₄Pd (991.08): C 63.01, H 4.98, P 12.50, Pd 10.73; found: C 62.45, H 4.95, P 12.29, Pd 10.17. IR (Nujol, KBr disks): $\tilde{\nu}$ = 1909 (νPd–H), 870, 818, 743, 694 cm⁻¹ (CH₂ rocking vibrations of diphosphane ligands); ¹H NMR (400.13 MHz, CD₂Cl₂, 225 K): δ = -7.22 (q, ²J_{H-P} = 53.7 Hz, H), 2.27 (br, CH₂), 7.16 (br, *o*), 7.22 (dd, ³J_{m,p} = ³J_{m,o} = 7.3 Hz, *m*-dppe), 7.39 ppm (t, ³J_{p,m} = 7.3 Hz, *p*-dppe); ¹³C{¹H} NMR (CD₂Cl₂, 225 K): δ = 68.3 (s, CH₂), 129.3 (s, *p*-dppe), 131.0 (s, *m*-dppe), 132.5 (s, *o*-dppe), 133.1 ppm (d, ¹J_{C-P} = 43.6 Hz, C_{ipso}); ¹⁹F NMR (CD₂Cl₂, 225 K): δ = -152.9 (br, ¹⁰BF₄), -153.0 ppm (br, ¹¹BF₄); ³¹P NMR (CD₂Cl₂, 225 K): δ = 34.09 ppm (d, ²J_{H-P} = 53.7 Hz, P).

Reaction of 1 with PhMgBr (6): PhMgBr (0.025 mmol), prepared from PhBr and Mg in anhydrous THF, was added to a yellow solution of 1 (26 mg, 0.024 mmol) in anhydrous THF (2 mL) under dinitrogen at 293 K with stirring. The solution immediately turned orange and then slowly yellow, while MgBr(CF₃SO₃) precipitated as a white solid. Quantitative formation of benzene was determined by GC-MS. [Pd(dppe)]₂ was characterized by IR, ¹H and ³¹P{¹H} NMR spectroscopy, by comparison with an authentic sample, and elemental analysis.

Reaction of 1 with (CH₃)₃C⁺CF₃SO₃⁻ (4): (CH₃)₃CCl (2 μL, 0.018 mmol) was added to a solution of CF₃SO₃Ag (4.6 mg, 0.018 mmol) in anhydrous THF (1 mL) under dinitrogen at 293 K. The solid AgCl that formed was filtered off. (CH₃)₃C⁺CF₃SO₃⁻ in THF was then added to a yellow solution of 1 (18 mg, 0.017 mmol) in anhydrous THF (1.5 mL) under dinitrogen at 293 K with stirring. The solution immediately turned white and [Pd(dppe)]₂(CF₃SO₃)₂ precipitated as a white solid. The ¹H NMR analysis of the solution and gas phase showed quantitative formation of isobutane. [Pd(dppe)]₂(CF₃SO₃)₂ was characterized by IR, ¹H and ³¹P{¹H} NMR spectroscopy, by comparison with an authentic sample, and elemental analysis.

Reaction of 1 with Ph₃C⁺CF₃SO₃⁻ (4′): A solution of Ph₃C⁺CF₃SO₃⁻ was prepared by addition of Ph₃CCl (3.9 mg, 0.014 mmol) to a solution of CF₃SO₃Ag (3.6 mg, 0.014 mmol) in THF and added to a solution of 1 (17.7 mg, 0.014 mmol) in THF (1 mL). [Pd(dppe)]₂(CF₃SO₃)₂ (3) precipitated as a white solid, and Ph₃CH (5) was detected in the solution by ¹H NMR spectroscopy.

Reaction of PhMgBr (6) with (CH₃)₃C⁺CF₃SO₃⁻ (4): (CH₃)₃CCl (3.3 μL, 0.030 mmol) was added to a solution of CF₃SO₃Ag (8 mg, 0.031 mmol) in anhydrous THF (1 mL) under dinitrogen at 293 K. Solid AgCl formed and was filtered off. To the clear solution, PhMgBr (0.031 mmol) in THF was added under dinitrogen at 293 K with stirring. The GC-MS analysis of the reaction solution and equilibrium gas phase showed the quantitative formation of benzene and isobutene in equimolar amounts.

Reaction of PhMgBr (6) and (CH₃)₃C⁺CF₃SO₃⁻ (4) in the presence of 1: (CH₃)₃CCl (1 μL, 0.009 mmol) was added to a solution of CF₃SO₃Ag (2.6 mg, 0.010 mmol) in anhydrous THF (1 mL) under dinitrogen at 293 K. The AgCl that formed was filtered off. The resulting solution and PhMgBr in THF (0.009 mmol) were simultaneously added to a yellow solution of 1 (9.8 mg, 0.009 mmol) in anhydrous THF (1 mL) under dinitrogen at 293 K with vigorous stirring. The resulting solution and the gas phase were analyzed by ¹H NMR spectroscopy and GC-MS and shown to contain benzene and isobutene.

Reaction of PhMgBr (6) and Ph₃C⁺CF₃SO₃⁻ (4) in the presence of 1′: Ph₃CCl (6.4 mg, 0.023 mmol) was added to CF₃SO₃Ag (6 mg, 0.023 mmol) in THF (1 mL). The filtered resulting solution and PhMgBr in THF (0.023 mmol) were simultaneously added to a solution of 1′ (26 mg, 0.023 mmol) in anhydrous THF (1 mL) under dinitrogen at 293 K with vigorous stirring. The resulting solution was analyzed by ¹H NMR spectroscopy and GC-MS and shown to contain benzene and triphenylmethane.

Reaction of 1 with CH₂=CHC(O)OMe (9): CH₂=CHC(O)OMe (1 μL, 0.011 mmol) was added to a solution of 1 (23.6 mg, 0.022 mmol) in anhydrous THF (2 mL) under dinitrogen at 293 K with stirring. [Pd(dppe)]₂(CF₃SO₃)₂ precipitated as white solid that was filtered off. A yellow solution of [Pd(dppe)]₂ in THF was also obtained. The methyl propionate that formed was monitored by ¹H NMR spectroscopy and GC-MS, and by comparison with an authentic sample.

General procedure for monitoring reactions by ¹H NMR (500 MHz, CD₂Cl₂, 293 K) and ³¹P{¹H} NMR (202.48 MHz, CD₂Cl₂, 293 K) spectroscopy: A water-free solution of 1 (0.023 mmol) in CD₂Cl₂ (0.75 mL) was prepared under dinitrogen in an NMR tube. PhMgBr, (CH₃)₃C⁺CF₃SO₃⁻ or methyl acrylate was added in an equimolar amount, the tube was sealed and the solution continuously monitored by ¹H and ³¹P{¹H} NMR spectroscopy at 293 K until no further change in the spectrum was observed.

Hydrogenation reactions: A fixed amount of the PdH catalyst (1, 1′ or 1′′) or Pd/C 5% (see Table 1) was added to a solution of cyclohexen-2-one in THF (3 mL) under dinitrogen in a glass reactor. When H₂ was used, the glass reactor was placed in an autoclave and 4 MPa of hydrogen was charged. The reaction mixture was heated at a fixed temperature with stirring and monitored by GC-MS by drawing samples while the reaction was running. When 2-propanol was used, the relevant amount was added to the reaction mixture (see Table 1), and the solution was heated at a fixed temperature with stirring and monitored by GC-MS.

Acknowledgement

The Italian authors thank the MIUR (Projects no. MM03027791 and 2002031332). The OTKA F037345 grant and computer time from NIIF Supercomputer Center are acknowledged by the Hungarian authors.

- [1] A. Dedieu, *Transition Metal Hydrides: Recent Advances in Theory and Experiments*, VCH, New York, 1991.
- [2] N. Sarker, J. W. Bruno, *J. Am. Chem. Soc.* **1999**, *121*, 2174–2180.
- [3] J. A. M. Simões, J. L. Beauchamp, *Chem. Rev.* **1990**, *90*, 629–688.
- [4] R. Ciancanelli, B. C. Noll, D. L. DuBois, M. R. DuBois, *J. Am. Chem. Soc.* **2002**, *124*, 2984–2992.

- [5] D. D. M. Wayner, V. D. Parker, *Acc. Chem. Res.* **1993**, *26*, 287–294.
- [6] a) D. L. DuBois, D. E. Berning, *Appl. Organomet. Chem.* **2000**, *14*, 860–862; b) D. E. Berning, B. C. Noll, D. L. DuBois, *J. Am. Chem. Soc.* **1999**, *121*, 11432–11447.
- [7] R. A. Schunn, *Inorg. Chem.* **1970**, *9*, 394–395.
- [8] M. Aresta, E. Quaranta, *J. Organomet. Chem.* **2002**, *662*, 112–119.
- [9] M. Aresta, A. Dibenedetto, E. Amodio, I. Pápai, G. Schubert, *Inorg. Chem.* **2002**, *41*, 6550–6552.
- [10] A. Macchioni, *Eur. J. Inorg. Chem.* **2003**, 195–205, and references therein.
- [11] a) A. Macchioni, C. Zuccaccia, E. Clot, K. Gruet, R. H. Crabtree, *Organometallics* **2001**, *20*, 2367–2373; b) K. Gruet, E. Clot, O. Eisenstein, D. H. Lee, B. Patel, A. Macchioni, R. H. Crabtree, *New J. Chem.* **2003**, *27*, 80–87.
- [12] The intensity of a NOE cross peak due to N_I equivalent spins I and N_S equivalent spins S is proportional to the ratio $N_I N_S / (N_I + N_S)$: S. Macura, R. R. Ernst, *Mol. Phys.* **1980**, *41*, 95–117.
- [13] J. Price, R. Ciancanelli, B. C. Noll, C. J. Curtis, D. L. DuBois, M. Rakowski Dubois, *Organometallics* **2002**, *21*, 4833–4839.
- [14] Note that a number of other four-coordinate structures can be located on the $[\text{PdH}(\text{dpe})_2]^+$ potential energy surface as local minima because the molecule can easily undergo internal rotations about the P–C and C–C bonds. The relative stabilities of these minima, however, are very similar to that shown in Figure 4.
- [15] M. Aresta, A. Dibenedetto, E. Amodio, I. Tommasi, *Eur. J. Inorg. Chem.* **2002**, 2188–2193.
- [16] As we demonstrate later in this paper, **1** is able to hydrogenate an olefin. However, the hydrogenation reaction is slower than the single hydride- or proton-transfer reaction.
- [17] a) ADF2000.02, SCM, Theoretical Chemistry, Vrije Universiteit, Amsterdam, The Netherlands, <http://www.scm.com>, and references therein; b) C. C. Pye, T. Ziegler, *Theor. Chem. Acc.* **1999**, *101*, 396–408.
- [18] I. Guibert, D. Neibecker, I. Tkatchenko, *J. Chem. Soc. Chem. Commun.* **1989**, 1850–1852.
- [19] R. Noyori, *Angew. Chem.* **2002**, *114*, 2108–2123; *Angew. Chem. Int. Ed.* **2002**, *41*, 2008–2022.
- [20] D. D. Perrin, W. L. F. Armarego, D. R. Perrin, *Purification of Laboratory Chemicals*, Pergamon, Oxford, England, **1986**.
- [21] X. Lopez, M. Schaefer, A. Dejaegere, M. Karplus, *J. Am. Chem. Soc.* **2002**, *124*, 5010–5018.
- [22] M. Bail, C. K. Schauer, T. Ziegler, *J. Am. Chem. Soc.* **2002**, *124*, 11167–11181.
- [23] From test calculations carried out for protonation reactions investigated in: R. J. Angelici, *Acc. Chem. Res.* **1995**, *28*, 51–60.
- [24] J. Jeener, B. H. Meier, P. Bachmann, R. R. Ernst, *J. Chem. Phys.* **1979**, *71*, 4546–4553.
- [25] R. Wagner, S. Berger, *J. Magn. Reson. Ser. A* **1996**, *123*, 119–121.
- [26] B. Lix, F. D. Sönnichsen, B. D. Sykes, *J. Magn. Reson. Ser. A* **1996**, *121*, 83–87.

Received: February 23, 2004
Published online: June 9, 2004